

Phase matched scanning optical parametric chirped pulse amplification based on pump beam deflection

Rong Ye(叶荣), Huining Dong(董会宁), Xianyun Wu(吴显云), and Xiang Gao(高翔)
Citation: Chin. Phys. B, 2021, 30 (**10**): 104209. DOI: 10.1088/1674-1056/abfbda
Journal homepage: http://cpb.iphy.ac.cn; http://iopscience.iop.org/cpb

What follows is a list of articles you may be interested in

A two-mode squeezed light based on a double-pump phase-matching geometry

Xuan-Jian He(何烜坚), Jun Jia(贾俊), Gao-Feng Jiao(焦高锋), Li-Qing Chen(陈丽清), Chun-Hua Yuan(袁春华), Wei-Ping Zhang(张卫平)
Chin. Phys. B, 2020, 29 (**7**): 074207. DOI: 10.1088/1674-1056/ab8abd

Effect of dark soliton on the spectral evolution of bright soliton in a silicon-on-insulator waveguide

Zhen Liu(刘振), Wei-Guo Jia(贾维国), Hong-Yu Wang(王红玉), Yang Wang(汪洋), Neimule Men-Ke(门克内木乐), Jun-Ping Zhang(张俊萍)
Chin. Phys. B, 2020, 29 (**6**): 064212. DOI: 10.1088/1674-1056/ab84d9

Refractive index sensor based on high-order surface plasmon resonance in gold nanofilm coated photonic crystal fiber

Zhen-Kai Fan(范振凯), Shao-Bo Fang(方少波), Shu-Guang Li(李曙光), Zhi-Yi Wei(魏志义)
Chin. Phys. B, 2019, 28 (**9**): 094209. DOI: 10.1088/1674-1056/ab327a

Analysis of third and one-third harmonic generation in lossy waveguides

Jianyu Zhang(张剑宇), Yunxu Sun(孙云旭), Qinghai Song(宋清海)
Chin. Phys. B, 2019, 28 (**6**): 064206. DOI: 10.1088/1674-1056/28/6/064206

Propagation characteristics of oblique incidence terahertz wave through non-uniform plasma

Antao Chen(陈安涛), Haoyu Sun(孙浩宇), Yiping Han(韩一平), Jiajie Wang(汪加洁), Zhiwei Cui(崔志伟)
Chin. Phys. B, 2019, 28 (**1**): 014201. DOI: 10.1088/1674-1056/28/1/014201

Phase matched scanning optical parametric chirped pulse amplification based on pump beam deflection*

Rong Ye(叶荣)[1,†], Huining Dong(董会宁)[1], Xianyun Wu(吴显云)[1], and Xiang Gao(高翔)[2]

[1] College of Physics and Engineering, Chengdu Normal University, Chengdu 611130, China
[2] College of Science, Southwest University of Science and Technology, Mianyang 621010, China

(Received 4 February 2021; revised manuscript received 22 April 2021; accepted manuscript online 27 April 2021)

Combined with the optical beam deflection, a novel approach of phase matched broadband scanning optical parametric chirped pulse amplification (OPCPA) was proposed. For this scheme, there was no superfluous operations to the chirped signal pulse which propagated in a changeless direction straightforward, but the pump beam were deflected in space with time by passing through a KTN crystal, which was applied with varied driving voltage. The theories of phase matching of each chirped signal frequency based on pump beam deflection was analyzed detailedly. And the type-I amplification of chirped signal with 800 nm central wavelength and 20 nm bandwidth pumped by 532 nm in BBO crystal was simulated as a case in point. The simulation results showed that the spectral distribution of chirped signal pulse was almost the same as the initial form, i.e., there was nearly no narrowing on the amplified spectrum by using of the scanning OPCPA based on pump beam deflection. In addition, the simulations demonstrated that it was worth minimizing the voltage deviation applied to KTN crystal as much as possible for the sake of better waveform, larger bandwidth and higher conversion efficiency of amplified signal pulse in the proposed scanning OPCPA.

Keywords: optical parametric chirped pulse amplification, optical beam deflection, phase matching, scanning, KTN crystal

PACS: 42.65.−k, 42.70.Mp, 42.65.Re, 42.79.Ls **DOI:** 10.1088/1674-1056/abfbda

1. Introduction

The broadband phase matching is still a problem that has not been solved well for optical parametric chirped pulse amplification (OPCPA), although the peak power of ultra-short laser pulse has been increased to terawatt (TW, 10^{12} W), petawatt (PW, 10^{15} W) and even exawatt (EW, 10^{18} W) in virtue of the OPCPA, whose focused intensity is near to 10^{23}–10^{24} W/cm^2.[1–4] There is no denying that the OPCPA is the preferred technology to output PW high power pulse at present. And in recent years, high average power, kinds of parametric crystal and multi-wavelength regions from visible to near-infrared, even mid-infrared have been widely demonstrated around the world.[5–7] Although the bandwidth of the signal pulse in spectral domain wider and the compressed duration shorter such as few-cycle in time domain, the limited gain bandwidth cannot ensure that it is phase matched for each frequency component of the signal pulse. And some research indicate that the intrinsic phase-mismatch induces the optical parametric phase which degrades the bandwidth of the amplified signal pulse.[8] To further enhance the phase matching and amplified bandwidth, some measures have been explored, for instance, achromatic phase or quasi-phase matching OPCPA.[9–11] Actually, too much operation to the signal pulse is undesired because the tilted pulse front or wave front caused by dispersion elements may induce the beam quality variation and so on. However, the OPCPA, predictably, is becoming most widely used in the whole table, high-power and high-energy ultra-short laser pulse system step by step.

2. Theoretical basis of phase-matched scanning OPCPA

In the second order nonlinear optical effects of OPCPA, the weak signal pulse obtains amplified energy from the robust pump pulse, and this process produces addition idler pulse. Generally, the chirped signal pulse whose frequency shows linear change with time is broadened from ultra-short laser pulse by stretcher. Although there are two main geometry schemes, i.e., collinear and non-collinear optical parametric amplification, the second one is widely adopted inasmuch as the interactional three waves leave from the nonlinearity crystal in different directions without any splitting system and the group velocity of the three pulse is easier matched in a large wavelength range in the non-collinear amplification. The efficiency of parametric conversion usually depends on the phase matching which is also known as the conservation of momentum in optics. The gain and conversion efficiency is the highest when the three waves are phase matched completely and the amplified signal spectrum is wide enough to support the

*Project supported by Science and Technology Innovation Seedling Project of Sichuan Province, China (Grant No. 2018100) and Major Project of CDNU (Grant No. CS18ZDZ0511).

†Corresponding author. E-mail: yj1987211@163.com

© 2021 Chinese Physical Society and IOP Publishing Ltd

compressed ultra-short durations for Fourier transform limited pulse. Though the parametric amplification is also capable in the case of three coupling waves phase-mismatched, the gain and conversion efficiency will decrease obviously. By ignoring the vertical mismatch on the premise of small non-collinear angle, the phase-mismatching Δk along the pumping direction is

$$\Delta \boldsymbol{k} = \boldsymbol{k}_{\rm p} - \boldsymbol{k}_{\rm s}\cos\alpha - \boldsymbol{k}_{\rm i}\cos\beta, \tag{1}$$

where $\boldsymbol{k}_j$ (j = p, s, and i refers to the bump, signal and idler pulse, respectively) is the wave-vector. The non-collinear angle α is the angle between the pump wave-vector and the signal wave-vector, which is linked with β between the pump and idler wave, described as

$$\beta = \arcsin\left(\frac{n_{\rm s}\omega_{\rm s}}{n_{\rm i}\omega_{\rm i}}\sin\alpha\right). \tag{2}$$

Actually, for broadband signal range, $\Delta k = 0$, < 0 or > 0 is all possible which depends on the signal wavelength, non-collinear angle, and phase-matching angle $\theta_{\rm m}$. The phase-matching angle $\theta_{\rm m}$ is the angle between the pump beam and the optical-axis, expressed as

$$\theta_{\rm m} = \arcsin\left\{\frac{n_{\rm op}^2 n_{\rm ep}^2\lambda_{\rm s}^2\lambda_{\rm i}^2 - n_{\rm ep}^2\left[n_{\rm s}^2\lambda_{\rm p}^2\lambda_{\rm i}^2 + n_{\rm i}^2\lambda_{\rm p}^2\lambda_{\rm s}^2 + 2n_{\rm s}n_{\rm i}\lambda_{\rm p}^2\lambda_{\rm s}\lambda_{\rm i}\cos(\alpha+\beta)\right]}{(n_{\rm op}^2 + n_{\rm ep}^2)\left[n_{\rm s}^2\lambda_{\rm p}^2\lambda_{\rm i}^2 + n_{\rm i}^2\lambda_{\rm p}^2\lambda_{\rm s}^2 + 2n_{\rm s}n_{\rm i}\lambda_{\rm p}^2\lambda_{\rm s}\lambda_{\rm i}\cos(\alpha+\beta)\right]}\right\}, \tag{3}$$

where $n_{\rm op}$ and $n_{\rm ep}$ are the main refractive indexes of pump light in crystal, supposed type-I ($e_{\rm p} = o_{\rm s} + o_{\rm i}$) parametric amplification.

We take the β-BaB_2O_4(BBO) crystal as an example. For the central 800 nm wavelength signal pumped by 532 nm, the absolute phase-matching angle $\theta_{\rm m0}$ supporting $\Delta k = 0$ are approximately 26.85° and 29.34°, with the non-collinear angle $\alpha_0 = 4°$ and 5° correspondingly. However, the actual signal pulse has a certain bandwidth, and namely it is difficult to achieve the whole phase matching on the condition of constant geometric angle $\theta_{\rm m0}$.

According to the above discussion, the contour plots of the phase-mismatching Δk, signal wavelength $\lambda_{\rm s}$ and phase-matching angle $\theta_{\rm m}$ are illustrated in Fig. 1(a). There are two contour lines, thin and thick, which are plotted with different central phase-matching angle $\theta_{\rm m0}$ and corresponding central non-collinear angle α_0 for more intuitively. Firstly, it is obvious that different signal wavelength occurs different phase-mismatching Δk with variable $\theta_{\rm m}$. Secondly, for the sake of phase matching of each signal wavelength, exclusive $\theta_{\rm m}$ is essential to support the phase-matching $\Delta k = 0$ line. Furthermore, from the characteristics of the $\Delta k = 0$ line we note that the needed $\theta_{\rm m}$ varies almost linearly with signal wavelength in near 100 nm wide range, which suggests the angle changing rate $D_{\theta \rm m}$ is equivalent to the slope of the phase-matching line. Last but not least, for broadband phase matching as shown in Fig. 1(b) the non-collinear angle α also changes synchronous with $\theta_{\rm m}$, but the angle γ between signal beam and the optical-axis of crystal is constant 22.85° and 24.34° for the thin and thick contour lines, respectively, i.e., the direction of signal beam does not change and is invariable throughout the amplification.

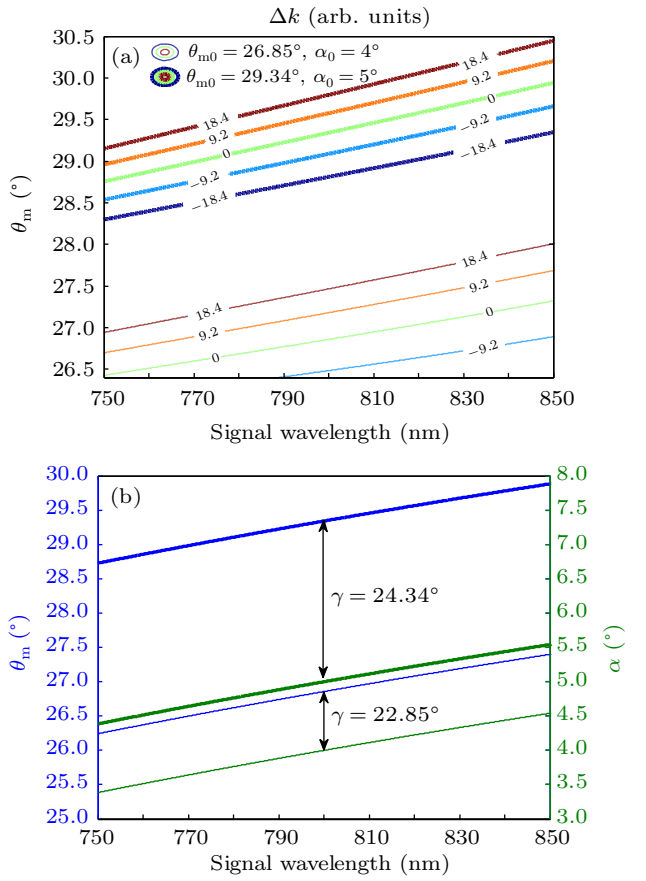


Fig. 1. (a) The contour plots of the phase-mismatching Δk, signal wavelength $\lambda_{\rm s}$ and phase-matching angle $\theta_{\rm m}$. The thin and thick contour lines are presented with different central phase-matching angle $\theta_{\rm m0}$ and central non-collinear angle α_0. (b) Variation of $\theta_{\rm m}$ and α with signal wavelength in the best phase matching performance where $\gamma = \theta_{\rm m} - \alpha$.

From the above discussion, it is feasible to enable each signal wavelength phase matching whenever possible by deflecting the pump beam with time for the purpose of entering into the nonlinear crystal with variational $\theta_{\rm m}$. And the geometry relationship of three wave-vectors phase matching is depicted in Fig. 2(a). It illustrates that the wave-vector of signal $k_{\rm s}$, pump $k_{\rm p}$ and the corresponding idler $k_{\rm i}$ form a vector

triangle always when the pump beam deflects with time to satisfy the needed $\theta_{\rm m}$. Figure 2(b) is the block diagram view of the scanning OPCPA based on the pump beam deflection. The chirped signal pulse propagates in a changeless direction, and remains the angle γ unchanged. The pump pulse deflects in space with time by passing through a KTN crystal, which is applied voltage in the signal pulse duration. The variation of $\theta_{\rm m}$ with time is synchronous with it of signal wavelength, which makes for broadband phase matching and maximum amplified spectrum.

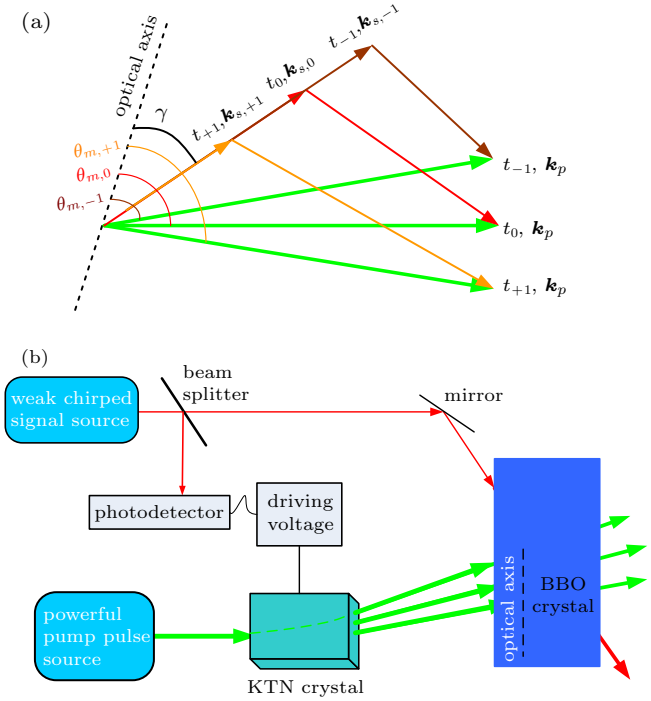


Fig. 2. (a) The phase-matching vector graph for non-collinear OPCPA in control of deflecting pump beam. (b) Schematic drawing of the scanning OPCPA based on pump beam deflection.

The cubic crystal KTN ($KTa_{1-x}Nb_xO_3$, potassium tantalate niobate) has excellent electro-optical properties, and its quadratic electro-optic coefficient is one of the largest among the known crystals. After the first successful experiment and mechanism exploration of optical deflection in KTN crystal based on the quadratic electro-optical effect, kinds of optical beam splitter, optical switch, multi-dimensional scanning and ns magnitudes response have been designed and implemented.[12–15] According to the previous analysis of phase matching issues, the deflected angle of pump beam transits KTN crystal, which is put on voltage in the proposed scanning OPCPA, is given as below:[16]

$$\Delta\theta_{\rm m} = \theta_{\rm m} - \theta_{\rm m0} = -\frac{9Ln_0^3 s_{ij}}{8d}\left(\frac{U}{d}\right)^2, \tag{4}$$

where L and d are the length and thickness of the crystal, respectively. n_0 represents the linear refractive index, s_{ij} is the Kerr constant of the crystal, and often equals to 1.0×10^{-14} m^2/V^2. Because $\theta_{\rm m}$ varies almost linearly with signal wavelength in a broadband range by inspection of Fig. 1, the deflected angle changing rate $D_{\theta\rm m}$ is defined as

$$D_{\theta\rm m} = \frac{\Delta\theta_{\rm m}}{\Delta\lambda}, \tag{5}$$

which is exactly the slope of $\Delta k = 0$ line. Invoking the needed $\Delta\theta_{\rm m}$, it follows from Eq. (4) that the driving voltage U applied to the crystal can be written in the form

$$U = -\frac{\Delta\theta_{\rm m}}{|\Delta\theta_{\rm m}|}\sqrt{\frac{8\,|\Delta\alpha|\,d^3}{9Ln_0^3 s_{ij}}}. \tag{6}$$

Generally, in a moving coordinate system the coupled wave equations of type-I OPCPA in BBO crystal are written as[17]

$$\begin{cases} \dfrac{\partial E_{\rm s}}{\partial r} = -{\rm i}\dfrac{\omega_{\rm s} d_{\rm eff}}{n_{\rm s} c} E_{\rm p} E_{\rm i}^* \exp(-{\rm i}\Delta k r), \\ \dfrac{\partial E_{\rm i}}{\partial r} = -{\rm i}\dfrac{\omega_{\rm i} d_{\rm eff}}{n_{\rm i} c} E_{\rm p} E_{\rm s}^* \exp(-{\rm i}\Delta k r), \\ \dfrac{\partial E_{\rm p}}{\partial r} = -{\rm i}\dfrac{\omega_{\rm p} d_{\rm eff}}{n_{\rm p} c} E_{\rm s} E_{\rm i} \exp({\rm i}\Delta k r), \end{cases} \tag{7}$$

where E_j (j = p, s, i) is the electric field of three waves with second order nonlinear action. n_j and ω_j (j = p, s, i) refer to the refractive index and frequency of each pulse in the medium, respectively. $d_{\rm eff}$ is the second-order effective nonlinear coefficient.

3. Numerical simulation and discussion of scanning OPCPA

Taking into account the amplification of the signal and pump both as Gaussian pulses, the split-step Fourier and fourth order Runge–Kutta method are used to transform the mathematical model into a discrete simulation model, by using MATLAB2014a simulation software to simulate Eq. (7)'s dynastic performance. In this simulation, resulting of similar features, a specific case of central $\theta_{\rm m0} = 29.34^\circ$ corresponding to $\alpha_0 = 5^\circ$ for signal center wavelength $\lambda_{\rm s0} = 800$ nm is provided to show the scanning OPCPA with pump deflection. The length of nonlinear BBO crystal and deflection KTN crystal is $L_{\rm BBO} = 1.22$ mm, and $L_{\rm KTN} = 40$ mm, respectively. The linear chirped coefficient $C_{\rm s}$ of the signal pulse is 21230 corresponding to bandwidth approximately 20 nm, and the deflected angle changing rate $D_{\theta\rm m} = 0.0115$ °/nm. In addition, the signal pulse duration $T_{\rm ws} = 1$ ns with the peak intensity $I_{0\rm s} = 0.1$ MW/cm^2 and assuming monochromatic wavelength $\lambda_{\rm p} = 532$ nm of pump pulse whose pulse duration $T_{\rm wp}$ is 2 ns with peak intensity $I_{0\rm p} = 1$ GW/cm^2.

Figure 3 shows the amplified temporal profile and the spectral distribution of signal with proposed scanning OPCPA

in comparison to that without it. The initial chirped signal pulse shows Gaussian distribution whenever in time or frequency domain, and its bandwidth is almost 20 nm (FWHM). It is observed that after the traditional amplification of fixed phase matching angle, usually θ_{m0}, the waveform and spectrum of chirped signal are both narrowed, which is mainly caused by the phase-mismatching except the central wavelength. In contrast, on the strength of scanning OPCPA the amplified temporal profile and spectral distribution of signal pulse exhibit a good agreement with the initial ones, and it almost remains the original bandwidth unchanged under the aegis of phase matching of each signal wavelength. In addition, the conversion efficiency of the scanning amplified mode is approximately 27% in excess of the conventional 3%. This reflects the fact that it is entirely possible to broaden the phase matching bandwidth greatly and improve the gain of signal pulse adequately by means of scanning OPCPA based on pump deflection.

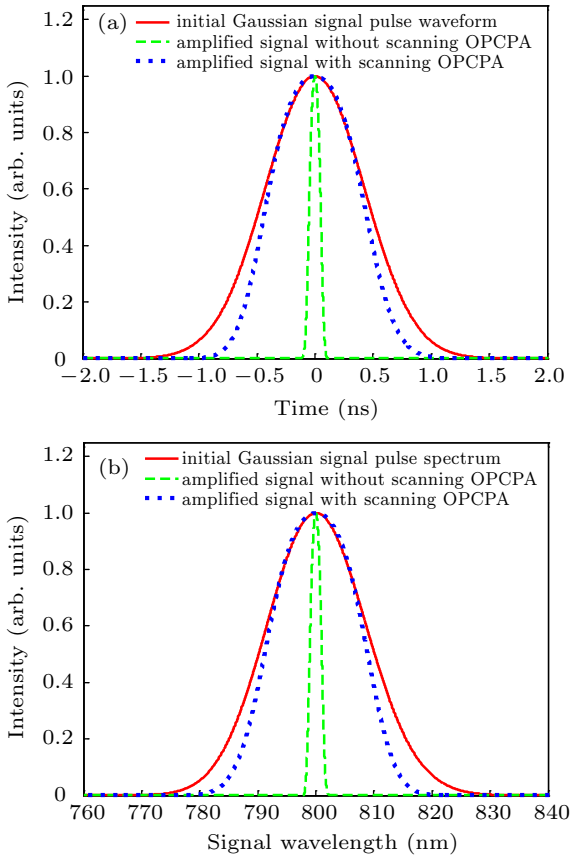


Fig. 3. Comparison of the amplified signal pulse waveform in time domain and frequency spectrum with the conventional and scanning amplification. (a) Temporal profile. (b) Spectral distribution.

In order to achieve the above-mentioned scanning OPCPA, the KTN crystal needs to be applied with an appropriate driving voltage, and the variation of the voltage with time is shown in Fig. 4(a). The pump beam deflects in space after passing through KTN crystal, and its deflection angle makes the most of phase matching $\Delta k = 0$ of each frequency component of chirped signal pulse, as the dashed line shown in Fig. 4(b). From the solid line perspective, the farther the off-center wavelength is, the larger the phase mismatch increase. That is because the fixed and just one phase-matched angle θ_{m0} contents phase matching of the central wavelength only, resulted in different phase mismatching for other signal wavelength.

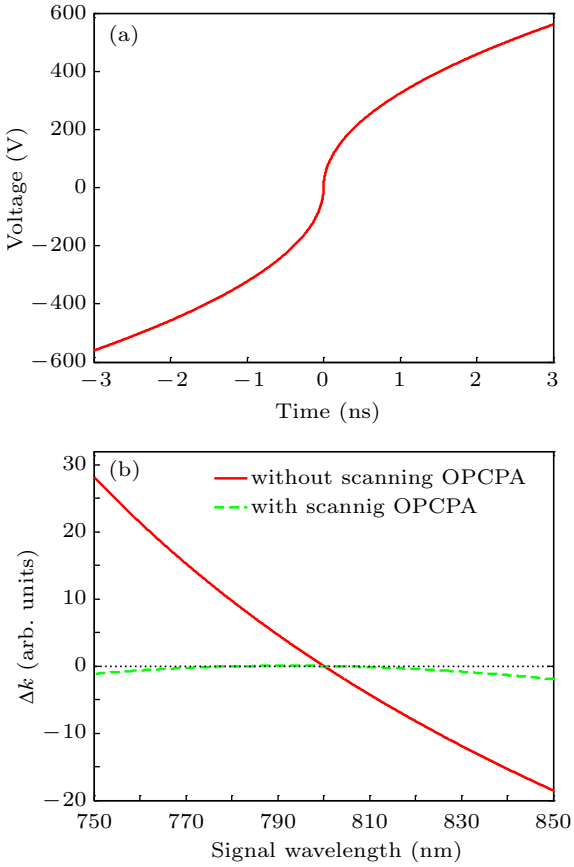


Fig. 4. The required voltage for pump beam deflection for scanning OPCPA and the comparison of phase mismatching with signal wavelength in the case of varied deflection θ_m and fixed constant θ_{m0}. (a) Required voltage. (b) Comparison of phase mismatching.

Figure 5 demonstrates the impact of unavoidable imperfection of actual driving voltage on the performance of scanning OPCPA. Obviously, as a result of the voltage deviation, the pump's deflected angle escapes from the optimal phase matching angle, which results in the distortion of amplified spectral distribution after the scanning OPCPA, and the greater the voltage deviation, the more serious the distortion is, as shown in Fig. 5(a). Furthermore, it is depicted in Fig. 5(b) that with the increasing of voltage deviation the energy extraction of signal from pump, i.e., the conversion efficiency decreases, whose main reason is the phase mismatching of each signal wavelength also caused by the voltage deviation. Accordingly to this end of obtaining amplified signal with better waveform, larger bandwidth and higher conversion efficiency, it is necessary to minimize the voltage deviation as much as possible. The voltage pulse applied to the KTN crystal can be

generated by any waveform generator.[18,19] The low energy signal pulse from the beam splitter can pass through the time delay line and then trigger the arbitrary waveform generator through the photodetector. In order to ensure the matching of variable voltage and deflection angle of pump light, the high precision time synchronization control technology is needed, and the time synchronization accuracy can reach the several picoseconds order, which can basically meet the needs of ns pulse amplification.[20,21]

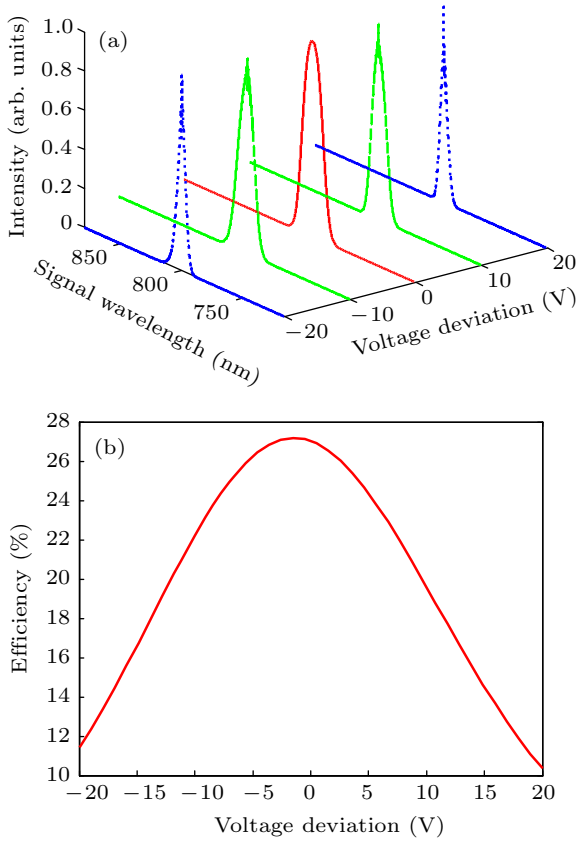


Fig. 5. The effect of voltage deviation on amplified signal spectrum and conversion efficiency after scanning OPCPA. (a) Signal spectrum evolution and (b) conversion efficiency with the voltage deviation.

4. Conclusions

In conclusion, the phase matching is the critical factors of OPCPA, and we first propose a novel scheme that broadens the bandwidth of phase-matched OPCPA combined with optical beam deflection. In this scheme, the chirped signal pulse propagates in a changeless direction, and there is no superfluous operations to it. The pump pulse are deflected in space with time by passing through a KTN crystal which is applied with varied driving voltage. By virtue of the deflection of pump beam, the phase matching angle θ_{m} is synchronous with the variation of signal wavelength in time domain, which provides broadband phase matching, spectral distribution and higher conversion efficiency. The amplification of chirped signal with 800 nm central wavelength and 20 nm bandwidth pumped by 532 nm is simulated. The results demonstrate that the amplified temporal profile and spectral distribution of signal pulse exhibit a good agreement with the initial ones, and it almost remains the original bandwidth unchanged by using of the scanning OPCPA based on the pump deflection. And it is worth minimizing the voltage deviation as much as possible for better waveform, larger bandwidth and higher conversion efficiency of amplified signal pulse.

References

[1] Danson C N, Haefner C, Bromage J, Butcher T, Chanteloup J F, Chowdhury E A, Galvanauskas A, Gizzi L A, Hein J, Hillier D I, Hopps N W, Katto Y, Khazanov E A, KODAMA r, Korn G, Li R X, Li Y T, Limpert J, Ma J G, Nam C H, Neely D, Papadopoulos D, Penman P R, Qian L J, Rocca J J, Shaykin A A, Siders C W, Spindloe C, Szatmari S, Trines R M G M, Zhu J Q, Zhu P and Zuegel J 2019 *High Power Laser Sci. Eng.* **7** 1

[2] Xu L, Yu L H, Chu Y X, Gan Z B, Liang X Y, Li R X and Xu Z Z 2015 *Chin. Phys. B* **24** 018704

[3] Dubietis A, Jonušauskas G and Piskarskas A 1992 *Opt. Commun.* **88** 437

[4] Bromage J, Bahk S W, Begishev I A, Dorrer C, Guardalben M J, Hoffman B N, Oliver J B, Roides R G, Schiesser E M, Shoup M J III, Spilatro M, Webb B, Weiner D and Zuegel J D 2019 *High Power Laser Sci. Eng.* **7** e4-1

[5] Windeler M K R, Mecseki K, Miahahri A, Robinson J S, Fraser J M, Fry A R and Tavella F 2019 *Opt. Lett.* **44** 4287

[6] Yu L H, Liang X Y, Xu L, Li W Q, Peng C, Hu Z G, Wang C, Lu X M, Chu Y X, Gan Z B, Liu X D, Liu Y Q, Wang X L, Lu H H, Yin D J, Leng Y X, Li R X and Xu Z Z 2015 *Opt. Lett.* **40** 3412

[7] Zou X, Li W K, Liang H K, Liu K, Qu S Z, Wang Q J and Zhang Y 2019 *Opt. Lett.* **44** 2791

[8] Zhou B J, Ma J G, Wang J, Tang D L, Xie G Q, Yuan P, Zhu H Y and Qian L J 2017 *Phy. Rev. A* **95** 033841

[9] Wang C, Leng Y X, Liang X Y, Zhao B Z and Xu Z Z 2005 *Opt. Commun.* **246** 323

[10] Mayer B W, Phillips C R, Gallmann L and Keller U 2014 *Opt. Express* **22** 20798

[11] Bigler N, Pupeikis J, Hrisafov S, Gallmann L, Phillips C R and Keller U 2018 *Opt. Express* **26** 6036

[12] Gong D W, Hao T, Tan L Y and Zhou Z X 2011 *Appl. Opt.* **50** 28

[13] Gong D W, Liang Y G, Ou W J, Wang J J, Wu Y, Liu B and Zhou Z X 2016 *Materials Research Bulletin* **75** 7

[14] Zhu W B, Chao J H, Chen C J, Yin S Z and Hoffman R C 2016 *Scientific Reports* **6** 33143

[15] Chao J H, Zhu W B, Wang C, Yao J, Yin S and Hoffman R C 2015 *Proc. SPIE* **9586** 95860T-1

[16] Nakamura K, Miyazu J, Sasaura M and Fujiura K 2006 *Appl. Phy. Lett.* **89** 131115

[17] Grace E J, Tsangarts C L and New G H C 2006 *Opt. Commun.* **261** 225

[18] Wang A B, Liu C B and Tian Y 2015 *Measurement & Control Technology* **34** 119 (in Chinese)

[19] Aleksey B R 2019 *Instruments* **3** 1

[20] Zhang Y Y, Li G Y, Fan W, Wang X C, Jiang Y E and Shi Z D 2016 *Laser & Optoelectronics Progress* **53** 081405

[21] Chen L Z, Wen S C, Wang Y W, Zhao C J, Qian L J and Fan D Y 2010 *IEEE Journal of Quantum Electronics* **46** 1354